VanBerkum, M. F. A., & Means, A. R. (1991) J. Biol. Chem. 266, 21488–21495.
Vorherr, T., James, P., Krebs, J., Enyedi, A., McCormick, D. J., Penniston, J. T., & Carafoli, E. (1990) Biochemistry 29, 355–365.
Walsh, M. P. (1985) Biochemistry 24, 3724–3730.
Zoller, M. J., Nelson, N. C., & Taylor, S. S. (1981) J. Biol. Chem. 256, 10837–10842.

Aminonaphthalenesulfonamides, A New Class of Modifiable Fluorescent Detecting Groups and Their Use in Substrates for Serine Protease Enzymes†

Saulius Butenas,‡,§ Thomas Orfeo,‡ Jeffrey H. Lawson,‡ and Kenneth G. Mann*,‡

Institute of Biochemistry, Vilnius-MTP, Lithuania, and Department of Biochemistry, University of Vermont College of Medicine, Burlington, Vermont 05405

Received January 21, 1992; Revised Manuscript Received March 24, 1992

ABSTRACT: A series of new compounds, 6-amino-1-naphthalenesulfonamides (ANSN), were used as fluorescent detecting groups for substrates of amidases. These compounds have a high quantum fluorescent yield, and the sulfonyl moiety permits a large range of chemical modification. Fifteen ANSN substrates with the structure (N^{α}-Z)Arg-ANSNR_1R_2 were synthesized and evaluated for their reactivity with 8 proteases involved in blood coagulation and fibrinolysis. Thrombin, activated protein C, and urokinase rapidly hydrolyzed substrates with monosubstituted sulfonamide moieties (R_1 = H). The maximum rate of substrate hydrolysis for acrylic substituents was observed when R_2 = C_4H_9 (*n*-butyl homologue). The hydrolysis rates for substrates with branched substituents were slower than their linear analogues. Monosubstituted (N^{α}-Z)Arg-ANSNR_1R_2 possessing cyclohexyl or benzyl groups in the sulfonamide moiety were hydrolyzed by these three enzymes at rates similar to that of the *n*-butyl homologue (except the cyclohexyl compound for u-PA). Factor Xa rapidly hydrolyzed substrates with short alkyl chains, especially when R_1 = R_2 = CH_3 or C_2H_5. Lys-plasmin and rt-PA demonstrated low activity with these compounds, and the best results were accomplished for monosubstituted compounds when R_2 = benzyl (for both enzymes). Factor VIIa and factor IXaβ exhibited no activity with these substrates. A series of 14 peptidyl ANSN substrates were synthesized, and their reactivity for the same 8 enzymes was evaluated. Thrombin, factor Xa, APC, and Lys-plasmin hydrolyzed all of the substrates investigated. Urokinase, rt-PA, and factor IXaβ exhibited reactivity with a more limited group of substrates, and factor VIIa hydrolyzed only one compound (MesD-LGR-ANSN$(C_2H_5)_2$). The substrate ZGGRR-ANSNH(cyclo-C_6H_{11}) showed considerable specificity for APC in comparison with other enzymes (k_{cat}/K_M = 19 300 M^{-1} s^{-1} for APC, 1560 for factor IIa, and 180 for factor Xa). This kinetic advantage in substrate hydrolysis was utilized to evaluate the activation of protein C by thrombin in a continuous assay format. Substrate (D-LPR-ANSNHC_3H_7) was used to evaluate factor IX activation by the factor VIIa/tissue factor enzymatic complex in a discontinuous assay. A comparison between the commercially available substrate chromozyme TH (*p*-nitroanilide) and the ANSN substrate with the same peptide sequence (TosGPR) demonstrated that aminonaphthalenesulfonamide increased the specificity (k_{cat}/K_M) of substrate hydrolysis by thrombin more than 30 times, with respect to factor Xa substrate hydrolysis.

The proteases involved in coagulation and fibrinolysis are trypsin-like serine proteases which preferentially hydrolyze peptide, ester, or amide bonds in which a basic amino acid provides the carbonyl group of the scissile bond. The specificity of enzyme/substrate interactions is a complex function of a variety of structural factors which include binding domains in the protease for specific amino acid side chains located on both the amino (P_1–P_n) and carboxyl (P_1'–P_n') side of the targeted lysine or arginine residue in the substrate protein.[1] The idea that short peptide substrates can be designed which incorporate enough information to discriminate among different proteases relies on the concept that each active site is comprised of a unique series of side chain binding "pockets".

A number of studies evaluating the utility of synthetic substrates for many of the proteases involved in blood coagulation and fibrinolysis have been reported (Cho et al., 1984; McRay et al., 1981; Lottenberg et al., 1981). Generally, these studies have evaluated the reactivity of substrates containing 4-nitroaniline and amides of 7-amino-4-methylcoumarins for this class of serine proteases. This work has provided a large amount of information regarding contributions of the P_1–P_3 amino acids in an attempt to optimize enzymatic substrate specificity for a particular protease. However, a design strategy employing structural variations of the detecting group

† This work was supported by National Institute of Health Grants HL35058, HL46973, HL46703, and HL07594 and by the Department of Biochemistry, University of Vermont.

* To whom correspondence should be addressed.
‡ University of Vermont College of Medicine.
§ Institute of Biochemistry, Vilnius-MTP.

[1] The nomenclature used to identify individual amino acid residues of the substrate (P_2, P_1, P_1', etc.) and the subsites of the enzyme (S_2, S_1, S_1', etc.) is that of Schechter and Berger (1967).

0006-2960/92/0431-5399$03.00/0

(P′) to provide added specificity to the substrate has not been adequately explored.[2]

A large number of fluorogenic substrates for proteolytic enzymes have been reported (Lottenberg et al., 1981; Bell et al., 1974; Nieuwenhuizen et al., 1977; Morita et al., 1977). In general, these substrates provide increased sensitivity over similar substrates designed to exploit absorbance changes between substrate and product. Important characteristics which have guided the design of fluorogenic substrates have included the following: minimal overlap of the fluorescence spectral properties of substrate and hydrolysis products, reasonable solubility of substrate and fluorescent product in aqueous buffer, low rates of nonenzymatic hydrolysis of substrates, and stability of the generated fluorescent product to both photo and chemical decomposition.

We report here on a new class of fluorescent detecting group, the aminonaphthalenesulfonamides (ANSN).[3] The presented synthetic scheme enables a variety of substitutions of the parent aminonaphthalenesulfonate molecule at the sulfonate moiety. This factor permits exploration of the influence of structural features of the substrate detecting group (P′) on enzymatic specificity. In the present study, a number of these detecting groups were synthesized, covalently linked to the carboxyl group of arginine or peptides with C-terminal arginine, and their specificity as substrates for a series of coagulation and fibrinolytic proteases was assessed. Furthermore, specific examples of substrates which are useful in evaluating the activation of protein C and factor IX are described.

Experimental Procedures

Materials and Methods. 1-Palmitoyl-2-oleoylphosphatidylserine (PS), and 1-palmitoyl-2-oleoylphosphatidylcholine (PC) were purchased from Sigma. Phospholipid vesicles (PCPS) composed of 75% PC and 25% PS or 100% PC were prepared as described (Higgins & Mann, 1983). All other reagents were of analytical grade.

Bovine thrombin (Lundblad et al., 1976), bovine factor Xa (Krishnaswamy et al., 1987), bovine activated protein C (APC) (Haley et al., 1989), and Lys-plasmin (Claeys et al., 1973) were prepared by previously reported methods. Human factor IX was prepared by previously reported methods (Lawson & Mann, 1991) and activated to human factor IXa by factor XIa, a gift from Dr. Steve Olson using the general methods of Lindquist et al. (1978). Recombinant human coagulation factor VIIa (rVIIa) was provided as a gift from Dr. Ulla Hedner, Novo Pharmaceuticals (Pedersen et al., 1989). Recombinant t-PA (activase) was provided as a gift from Genentech Inc. Two-chain urokinase was provided as a gift from Collaborative Research, Bedford, MA. Recombinant tissue factor was provided as a gift from Dr. Shu-Len Liu, Hyland Division, Baxter Healthcare Corp.

The concentrations of proteins used in this study were calculated using the following molecular weights (M_r) and extinction coefficients ($E_{280}^{0.1\%}$): bovine thrombin, 36700, 1.95 (Mann et al., 1981); human factor VII and VIIa 50000, 1.39 (Bajaj et al., 1981); human factor IXa, 45000, 1.40 (Lindquist et al., 1978); bovine factor Xa, 45300, 1.24 (Fujikawa & Davie, 1976); bovine APC, 52650, 1.37 (Kisiel & Davie, 1981); rt-PA, 72000, 2.0 (Rijken & Collen, 1981); Lys-plasmin, 82900, 1.7 (Barlow et al., 1984); two-chain urokinase, 54700, 1.36 (White & Barlow, 1970). The concentration of recombinant tissue factor was determined by amino acid analysis and provided by Baxter Hyland Inc.

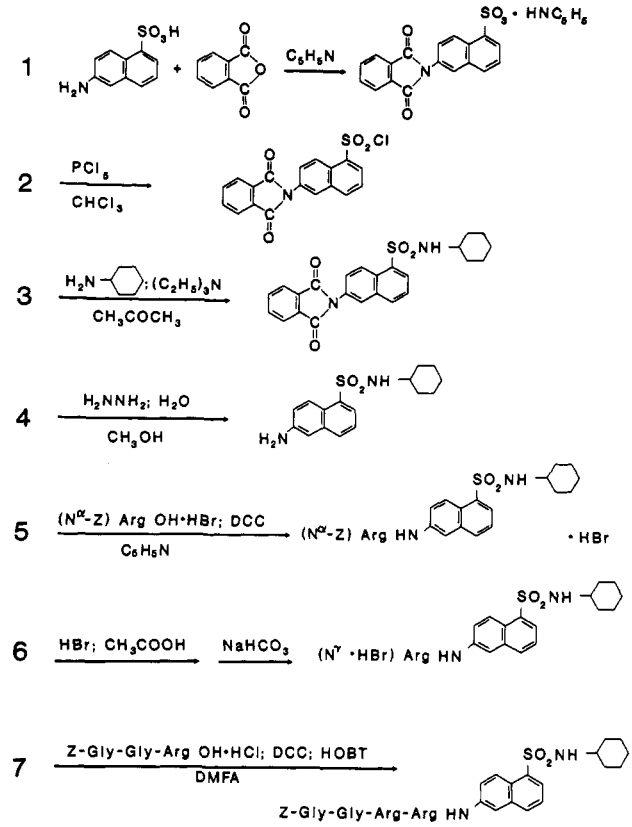

FIGURE 1: Synthetic scheme of the 6-((Z-Gly-Gly-Arg-Arg)-amino)-1-naphthalenecyclohexylsulfonamide. Abbreviations: DCC, 1,3-dicyclohexylcarbodiimide; HOBT, 1-hydroxybenzotriazole.

Synthesis of ANSNs. The ANSNs, peptides, and fluorogenic substrates were synthesized by Dr. S. Butenas and coworkers at the Institute of Biochemistry, Vilnius, Lithuania. The peptides were prepared according to methods of Anderson et al. (1964). In general, the synthetic scheme involves four steps: synthesis of ANSNs; synthesis of arginyl-ANSNs; synthesis of peptides; and synthesis of peptidyl-ANSNs. The complete synthesis for 6-((Z-Gly-Gly-Arg-Arg)amino)-1-naphthalenecyclohexylsulfonamide is presented below (see Figure 1).

(1) 6-Phthalimido-1-naphthalenesulfonic Acid Pyridinium Salt (I). A total of 223 g (1 mol) of 6-amino-1-naphthalenesulfonic acid and 148 g (1 mol) of phthalic anhydride were boiled for 5 h in 1 L of pyridine. After boiling, the reaction mixture was left at room temperature for 16 h. The precipitated product was filtered and washed with pyridine and water, and then the product was recrystallized from boiling water: yield 298 g (69%); mp 234–237 °C. Anal. Calcd. for $C_{23}H_{16}N_2SO_5$: C, 63.88; H, 3.73; N, 6.48; S, 7.42. Found: C, 63.74; H, 3.81; N, 6.52; S, 6.99.

(2) 6-Phthalimido-1-naphthalenesulfonyl Chloride (II). A total of 43.2 g (0.1 mol) of 6-phthalimido-1-naphthanenesulfonic acid pyridinium salt (I) and 62.5 g (0.3 mol) of phosphorus pentachloride were boiled for 5 h in 600 mL of chloroform. Solvent and the $POCl_3$ formed in the reaction were evaporated in a vacuum. The remaining product was added to 2 L of ice water, and after 1 h the precipitated product was filtered, washed with water, dried, and recrystallized from toluene: yield 36.8 g (99%); mp 248–251 °C.

[2] P′ is used to designate the position of the substrate detecting group with respect to the nomenclature of Schechter and Berger (1967).

[3] Abbreviations: Mes, methanesulfonyl; Z, carbobenzyloxy; Tos, *p*-toluenesulfonyl; p-NA, *p*-nitroanilide; DCC, 1,3-dicyclohexylcarbodiimide; ANSN, 6-amino-1-naphthalenesulfonamide; DMSO, dimethyl sulfoxide; DMFA, dimethylformamide; Boc, *tert*-butoxycarbonyl; Bz, benzoyl.

Table I: Physicochemical Constants for $ANSNR_1R_2$

	R_1	R_2	yield (%)	mp (°C)	R_f[a]	anal. data[b] C	H	N	S	formula	MW	emission maximum (nm)	rel. fluorescence[c]
IV	H	CH_3	57	145–148	0.38	56.10	5.16	11.96	13.11	$C_{11}H_{12}N_2SO_2$	236.2	468	92
						55.91	5.12	11.85	13.57				
V	H	C_2H_5	83	109–113	0.55	57.72	5.72	11.40	12.57	$C_{12}H_{14}N_2SO_2$	250.31	466	78
						57.58	5.64	11.19	12.81				
VI	H	C_3H_7	48		0.61	59.26	6.27	10.73	11.70	$C_{13}H_{16}N_2SO_2$	264.34	470	93
						59.07	6.10	10.60	12.13				
VII	H	i-C_3H_7	78	140–144	0.51	58.88	6.09	10.58	12.04	$C_{13}H_{16}N_2SO_2$	264.34	468	76
						59.07	6.10	10.60	12.13				
VIII	H	C_4H_9	46	76–79	0.48	60.56	6.45	10.20	11.37	$C_{14}H_{18}N_2SO_2$	278.37	467	63
						60.41	6.52	10.06	11.52				
IX	H	i-C_4H_9	79	48–50	0.57	60.40	6.62	9.93	11.02	$C_{14}H_{18}N_2SO_2$	278.37	468	100
						60.41	6.52	10.06	11.52				
X	H	t-C_4H_9	69	198–200	0.55	60.47	6.56	10.14	11.26	$C_{14}H_{18}N_2SO_2$	278.37	465	112
						60.41	6.52	10.06	11.52				
XI	H	C_5H_{11}	66	87–90	0.62	61.72	6.86	9.40	10.92	$C_{15}H_{20}N_2SO_2$	292.40	469	90
						61.62	6.89	9.58	10.96				
XII	H	cyclo-C_6H_{11}	48	136–140	0.69	63.15	6.81	9.18	10.84	$C_{16}H_230N_2SO_2$	304.41	466	101
						63.13	6.62	9.20	10.53				
XIII	H	benzyl	64	148–150	0.67	65.52	5.19	8.82	9.21	$C_{17}H_{16}N_2SO_2$	312.39	467	75
						65.36	5.16	8.97	10.26				
XIV	CH_3	CH_3	81	92–94	0.63	57.56	5.66	11.30	12.00	$C_{12}H_{14}N_2SO_2$	250.31	472	65
						57.58	5.64	11.19	12.81				
XV	C_2H_5	C_2H_5	46	106–108	0.74	60.54	6.57	9.89	11.35	$C_{14}H_{18}N_2SO_2$	278.37	470	89
						60.41	6.52	10.06	11.52				
XVI		$(CH_2)_5$	71	140–143	0.78	62.16	6.21	9.57	10.81	$C_{15}H_{18}N_2SO_2$	290.38	473	68
						62.04	6.25	9.65	11.04				
XVII		$(CH_2)_6$	44	187–190	0.79	63.28	4.46	9.07	10.18	$C_{16}H_{20}N_2SO_2$	304.41	469	96
						63.13	6.62	9.20	10.53				
XVIII		morpholyl	74	80–83	0.63	57.34	5.67	9.72	10.74	$C_{14}H_{16}N_2SO_3$	292.36	476	41
						57.51	5.52	9.58	10.97				

[a] Ethyl acetate–chloroform 1:1. [b] The top value for each entry is the found value; the bottom value is the calculated value. [c] Measured in TBS, pH 7.4, 22 °C. Concentration of $ANSNR_1R_2$ = 1 μM. Fluorescence is expressed relative to ANSNH(i-C_4H_9). Excitation wavelength = 352 nm, emission wavelength = 470 nm.

Anal. Calcd. for $C_{18}H_{10}NSClO_4$: C, 58.15; H, 2.71; N, 3.77; S, 8.63; Cl, 9.53. Found: C, 58.02; H, 2.84; N, 3.73; S, 9.01; Cl, 9.32.

(*3*) *6-Phthalimido-1-naphthalenecyclohexylsulfonamide* (*III*). A total of 37.2 g (0.1 mol) of 6-phthalimido-1-naphthalenesulfonyl chloride (II) was added to a solution of 11.4 mL (0.1 mol) of cyclohexylamine and 13.9 mL (0.1 mol) of triethylamine in 500 mL of acetone over 5 min. The reaction mixture was stirred at 20 °C for 4 h. The acetone was evaporated, and the residual was added to 1 L of water. The product was filtered and washed with water, dried, and recrystallized from methanol: yield 40.9 g (94%); mp 206–209 °C. Anal. Calcd. for $C_{24}H_{22}N_2SO_4$: C, 66.34; H, 5.10; N, 6.45; S, 7.38. Found: C, 66.48; H, 5.07; N, 6.32; S, 7.14.

(*4*) *6-Amino-1-naphthalenecyclohexylsulfonamide* (*XII*). A total of 43.5 g (0.1 mol) of 6-phthalimido-1-naphthalenecyclohexylsulfonamide was boilded for 4.5 h in 500 mL of methanol possessing 4.9 mL (0.1 mol) of hydrazine monohydrate. The methanol was evaporated, and the residual was extracted 2 × 200 mL with boiling chloroform. The chloroform was evaporated, and the product was recrystallized from methanol: yield 16.7 g (55%); mp 136–140 °C. Anal. Calcd. for $C_{16}H_{20}N_2SO_2$: C, 63.13; H, 6.62; N, 9.20; S, 10.53. Found: C, 63.15; H, 6.81; N, 9.18; S, 10.84. Physicochemical constants for all the 6-amino-1-naphthalenesulfonamides (IV–XVIII) prepared by this method are given in Table I.

Synthesis of 6-L-Arginylamino-1-naphthalenesulfonamides Hydrobromides. (*5*) *6-((N$^{\alpha}$-(Carbobenzyloxy)-L-arginyl)-amino)-1-naphthalenecyclohexylsulfonamide Hydrobromide* (*XXVII*). A total of 3.89 g (0.01 mol) of N$^{\alpha}$-(carbobenzyloxy)-L-arginine hydrobromide and 3.04 g (0.01 mol) of 6-amino-1-naphthalenecyclohexylsulfonamide (XII) were dissolved in 15 mL of dry pyridine. Then, 30 mL of dry toluene was added to this solution. The toluene was evaporated in a vacuum, and the reaction mixture was cooled to −20 °C. A total of 2.68 g (0.013 mol) of a 1,3-dicyclohexylcarbodiimide solution in 6 mL of dry pyridine was added to the reaction mixture. The mixture was held at −20 °C for 30 min and then warmed to 4 °C for 1 h, followed by an increase in the temperature to 20 °C for 20 h with stirring. The precipitated dicyclohexylurea was filtered, the pyridine was evaporated in a vacuum, and the remaining oil was dissolved in 40 mL of 1-propanol–chloroform (1:3). This solution was washed by the following steps: 15 mL of water, 15 mL of saturated sodium chloride containing 1 mL of concentrated HCl, 15 mL of 2% ammonia in water, and 15 mL of water. The organic layer was dried over anhydrous Na_2SO_4, the solvents were evaporated, and the residual oil was hardened by grinding with dry toluene. The reaction product was filtered, washed with dry toluene, dry diethyl ether, and recrystallized from 1-propanol: yield 6.35 g (94%); mp 135–141 °C; R_f = 0.69 (1-butanol–acetic acid–water 4:1:2); $[\alpha]_D^{20}$ = −12.6° (c 1; CH_3OH). Anal. Calcd. for $C_{30}H_{39}N_6BrSO_5$: C, 53.33; H, 5.82; N, 12.44; Br, 11.83; S, 4.75. Found: C, 53.21; H, 5.96; N, 12.63; Br, 11.48; S, 4.32. Physicochemical constants for all the 6-((N$^{\alpha}$-(carbobenzyloxy)-L-arginyl)amino)-1-naphthalenesulfonamide hydrobromides (XIX–XXXIII) prepared by the same method are given in Table II.

(*6*) *6-(L-Arginylamino)-1-naphthalenecyclohexylsulfonamide Hydrobromide* (*XLIV*). A total of 6.76 g (0.01 mol) of 6-((N$^{\alpha}$-(carbobenzyloxy)-L-arginyl)amino)-1-naphthalenecyclohexylsulfonamide hydrobromide (XXVII) was dissolved in 10 mL of 3 N HBr in glacial acetic acid and kept at room temperature for 2 h. The reaction mixture was added to 100 mL of dry diethyl ether. After 10 min the precipitate was filtered, washed with diethyl ether, and dried.

Table II: Physicochemical Constants for HBr·(N^{α}-Z)Arg-ANSNR$_1$R$_2$

	R_1	R_2	yield (%)	mp (°C)	$[\alpha]_D^{20}$ (c 1; CH_3OH)	R_f (BAW412)[a]	anal. data[b] C	H	N	S	Br	formula
XIX	H	CH_3	81	127–132	−13.3°	0.68	49.59	5.32	13.63	4.63	12.42	$C_{25}H_{31}N_6BrSO_5$
							49.42	5.14	13.83	5.28	13.15	
XX	H	C_2H_5	93	134–138	−14.1°	0.69	50.36	5.52	13.34	4.53	12.06	$C_{26}H_{33}N_6BrSO_5$
							50.24	5.35	13.52	5.10	12.86	
XXI	H	C_3H_7	94	118–124	−14.9°	0.71	51.21	5.61	13.62	4.29	11.72	$C_{27}H_{35}N_6BrSO_5$
							51.02	5.55	13.22	5.04	12.57	
XXII	H	i-C_3H_7	92	119–124	−14.3°	0.70	51.17	5.45	13.40	4.23	12.19	$C_{27}H_{35}N_6BrSO_5$
							51.02	5.55	13.22	5.04	12.57	
XXIII	H	C_4H_9	91	122–127	−14.6°	0.67	51.83	5.93	12.78	4.13	11.51	$C_{28}H_{37}N_6BrSO_5$
							51.77	5.74	12.94	4.94	12.30	
XXIV	H	i-C_4H_9	95	122–126	−13.5°	0.70	51.62	5.88	13.07	4.12	11.84	$C_{28}H_{37}N_6BrSO_5$
							51.77	5.74	12.94	4.94	12.30	
XXV	H	*t*-C_4H_9	20	145–148	−13.3°	0.55	51.92	5.81	12.85	4.63	12.03	$C_{28}H_{37}N_6BrSO_5$
							51.77	5.74	12.94	4.94	12.30	
XXVI	H	C_5H_{11}	91	120–124	−16.0°	0.77	52.58	6.13	12.85	4.42	11.89	$C_{29}H_{39}N_6BrSO_5$
							52.49	5.92	12.66	4.83	12.04	
XXVII	H	cyclo-C_6H_{11}	94	135–141	−12.6°	0.69	53.21	5.96	12.63	4.32	11.48	$C_{30}H_{39}N_6BrSO_5$
							53.33	5.82	12.44	4.75	11.83	
XXVIII	H	benzyl	96	161–164	−13.5°	0.63	54.58	5.25	12.14	4.23	10.93	$C_{31}H_{35}N_6BrSO_5$
							54.46	5.16	12.29	4.69	11.69	
XXIX	CH_3	CH_3	78	117–121	−13.4°	0.69	50.39	5.54	13.42	4.33	12.30	$C_{26}H_{33}N_6BrSO_5$
							50.24	5.35	13.52	5.16	12.85	
XXX	C_2H_5	C_2H_5	84	106–112	−12.8°	0.72	51.63	5.85	12.75	4.58	11.88	$C_{28}H_{37}N_6BrSO_5$
							51.77	5.74	12.94	4.94	12.30	
XXXI		$(CH_2)_5$	89	118–123	−12.8°	0.71	52.49	5.81	12.62	4.53	11.87	$C_{29}H_{37}N_6BrSO_5$
							52.65	5.64	12.70	4.85	12.08	
XXXII		$(CH_2)_6$	91	107–113	−13.8°	0.73	53.41	5.73	12.60	4.54	11.57	$C_{30}H_{39}N_6BrSO_5$
							53.33	5.82	12.44	4.75	11.83	
XXXIII		morpholyl	84	119–125	−12.3°	0.69	50.71	5.18	12.51	4.71	11.79	$C_{28}H_{35}N_6BrSO_6$
							50.68	5.32	12.66	4.83	12.04	

[a] BAW412 is 1-butanol–acetic acid–water 4:1:2. [b] The top value for each entry is the found value; the bottom value is the calculated value.

The dry 6-(L-arginylamino)-1-naphthalenecyclohexylsulfonamide dihydrobromide was dissolved in 10 mL of water, the solution was then poured into a separation funnel, and 50 mL of 1-butanol was added. This was followed by the addition of 5% $NaHCO_3$ with shaking until the water layer was pH 7.5. The organic layer was washed with water and then concentrated in a vacuum until the final volume of the solution was between 3 and 5 mL. The product was precipitated with dry diethyl ether, then filtered, washed with diethyl ether and dried: yield 4.82 g (89%); R_f = 0.43 (1-butanol–acetic acid–water 4:1:2); $[\alpha]_D^{20}$ = −2.0° (c 1; DMSO). Anal. Calcd. for $C_{22}H_{33}N_6BrSO_3$: C, 48.80; H, 6.14; N, 15.52; Br, 14.76; S, 5.92. Found: C, 48.94; H, 6.19; N, 15.48; Br, 15.01; S, 5.59. Physicochemical constants for all the 6-(L-arginylamino)-1-naphthalenesulfonamide hydrobromides (XXXIV–LVIII) are given in Table III.

Synthesis of 6-(Peptidylamino)-1-naphthalenesulfonamides. (*7*) *6-((Z-Gly-Gly-Arg-Arg)amino)-1-naphthalenecyclohexylsulfonamide* (*LII*). A total of 4.59 g (0.01 mol) of Z-Gly-Gly-Arg-OH hydrochloride, 2.68 g (0.013 mol) of 1,3-dicyclohexylcarbodiimide, and 1.35 g (0.01 mol) of 1-hydroxybenzotriazole hydrate were added to 25 mL of dry DMFA and cooled to −20 °C. The reaction mixture was kept at 0 °C for 1 h followed by the addition of 5.42 g (0.01 mol) of 6-(L-arginylamino)-1-naphthalenecyclohexylsulfonamide hydrobromide (XLIV) in 15 mL of dry DMFA. The reaction mixture was kept at 0 °C for 1 h and then warmed to 20 °C for 20 h with stirring. The precipitated dicyclohexylurea was filtered and the reaction solution was added to 150 mL of water. This solution was extracted 5 × 20 mL by a mixture of 1-butanol–ethyl acetate (1:1), and the organic layer was then washed with 3 × 7 mL of 5% $NaHCO_3$, 3 × 7 mL of 10% $KHSO_4$, and 3 × 7 mL of water. The organic layer was concentrated to a final volume of 3–5 mL and the product was precipitated with dry diethyl ether, filtered, washed with diethyl ether, and dried: yield 5.88 g (68%); R_f = 0.45 (1-butanol–acetic acid–water 4:2:1); $[\alpha]_D^{20}$ = −12.2° (c 1; DMSO). Physicochemical constants for all the peptide naphthalenesulfonamide substrates (XLIX–LXII) prepared by this method are given in Table IV.

Physical Characterization of the Synthesized Compounds. Melting points were determined on a Boetius melting point apparatus. Optical rotation measurements were performed on a Perkin-Elmer 141 polarimeter. Thin-layer chromatography was performed using aluminum oxide coated plates (VWR Scientific, Gibbstown, New Jersey).

Assay Methods. Enzyme assays were conducted in 20 mM Tris, 150 mM NaCl, pH 7.4 (TBS), at room temperature (22 °C). The final volume for all reaction mixtures was 2.0 mL. Fluorogenic substrates were dissolved in DMSO to a stock concentration of 10 mM. The 10 mM stock solution was diluted in TBS to the final working concentration prior to all assays. Enzyme was added to mixtures containing buffer components and substrate, and the rate of substrate hydrolysis was measured as the change in fluorescence over time, corresponding to the generation of the particular ANSN. Quantitation of substrate hydrolysis was accomplished by reference to standard curves constructed from the appropriate fluorescent moiety. Fluorescence was monitored (continuously or discontinuously) using a Perkin-Elmer fluorescence spectrophotometer, Model MPF-44A, equipped with a standard chart recorder. Fluorophore was detected using an excitation wavelength of 352 nm and emission wavelength of 470 nm with 8- and 12-nm slit settings, respectively. Light artifacts were minimized using a 399-nm long-pass cutoff filter in the emission light beam. Kinetic constants of substrate hydrolysis were determined using the nonlinear least-squares fitting program ENZFITTER (Elsevier-BIOSOFT, Cambridge, United Kingdom). This program was used to calculate the kinetic constants of substrate hydrolysis (k_{cat} and K_M) by iteratively

Table III: Physicochemical Constants for HBr·Arg-ANSNR$_1$R$_2$

	R_1	R_2	yield (%)	mp (°C)	$[\alpha]_D^{20}$ (c 1; DMSO)	R_f (BAW412)[a]	anal. data[b] C	H	N	S	Br	Brutto formula
XXXIV	H	CH_3	85	98–104	+3.3°	0.40	43.27	5.44	17.61	6.48	17.23	$C_{17}H_{25}N_6BrSO_3$
							43.13	5.32	17.75	6.77	16.88	
XXXV	H	C_2H_5	94	171–178	−4.1°	0.46	44.18	5.64	17.32	6.83	17.02	$C_{18}H_{27}N_6BrSO_3$
							44.36	5.58	17.24	6.58	16.39	
XXXVI	H	C_3H_7	95	133–138	−2.1°	0.41	45.68	5.96	16.84	6.11	16.35	$C_{19}H_{29}N_6BrSO_3$
							45.51	5.83	16.76	6.39	15.94	
XXXVII	H	i-C_3H_7	91	167–171	−1.0°	0.42	45.69	5.75	16.69	6.11	16.15	$C_{19}H_{29}N_6BrSO_3$
							45.51	5.83	16.76	6.39	15.94	
XXXVIII	H	C_4H_9	90	128–133	−2.0°	0.47	46.48	6.21	16.27	5.84	15.85	$C_{20}H_{31}N_6BrSO_3$
							46.60	6.06	16.30	6.20	15.50	
XXXIX	H	i-C_4H_9	96	161–165	−3.2°	0.47	46.68	5.94	16.38	6.12	16.11	$C_{20}H_{31}N_6BrSO_3$
							46.60	6.06	16.30	6.20	15.50	
XL	H	t-C_4H_9	85	163–168	−1.5°	0.33	46.76	6.21	16.14	5.96	15.88	$C_{20}H_{31}N_6BrSO_3$
							46.60	6.06	16.30	6.20	15.50	
XLI	H	C_5H_{11}	92	128–132	−5.0°	0.40	47.67	6.36	15.74	6.18	15.01	$C_{21}H_{33}N_6BrSO_3$
							47.63	6.28	15.87	6.05	15.09	
XLII	H	cyclo-C_6H_{11}	89	151–156	−2.0°	0.43	48.94	6.19	15.48	5.59	15.01	$C_{22}H_{33}N_6BrSO_3$
							48.80	6.14	15.52	5.92	14.76	
XLIII	H	benzyl	98	149–152	−1.0°	0.50	50.36	5.44	15.13	5.71	14.77	$C_{23}H_{29}N_6BrSO_3$
							50.27	5.32	15.29	5.83	14.54	
XLIV	CH_3	CH_3	83	99–102	+4.3°	0.41	44.18	5.72	17.11	6.12	16.24	$C_{18}H_{27}N_6BrSO_3$
							44.36	5.58	17.24	6.58	16.39	
XLV	C_2H_5	C_2H_5	92	133–137	−0.5°	0.44	46.51	6.18	16.14	6.56	15.12	$C_{20}H_{31}N_6BrSO_3$
							46.60	6.06	16.30	6.22	15.50	
XLVI	$(CH_2)_5$		90	124–130	−1.2°	0.48	47.68	6.06	15.84	5.82	15.55	$C_{21}H_{31}N_6BrSO_3$
							47.82	5.92	15.93	6.08	15.15	
XLVII	$(CH_2)_6$		89	135–139	−2.1°	0.50	48.73	6.28	15.70	5.41	15.03	$C_{22}H_{33}N_6BrSO_3$
							48.80	6.14	15.52	5.92	14.76	
XLVIII	morpholyl		81	154–159	+2.6°	0.38	45.39	5.67	16.03	5.54	15.81	$C_{20}H_{29}N_6BrSO_4$
							45.37	5.52	15.87	6.06	15.09	

[a] BAW412 is 1-butanol–acetic acid–water 4:1:2. [b] The top value for each entry is the found value; the bottom value is the calculated value.

Table IV: Physicochemical Constants for Peptidyl-ANSN

	substrates	MW	% yield	R_f[a]	$[\alpha]_D^{20}$[b]
XLIX	BocPFR-ANSNHC$_3$H$_7$	764.94	96	0.72	−12.8
L	PFR-ANSNHC$_3$h$_7$·2HCl	737.74	82	0.28	−6.8
LI	BocPPR-ANSNHC$_5$H$_{11}$	742.94	68	0.58	−27.8
LII	PPR-ANSNHC$_5$H$_{11}$·2HCl	715.74	84	0.33	−33.4
LIII	ZGGRR-ANSNH(cyclo-C$_6$H$_{11}$)	864.93	68	0.45	−12.2
LIV	GGRR-ANSNH(cyclo-C$_6$H$_{11}$)·3HBr	993.55	79	0.36	+4.2
LV	MesD-LGR-ANSN(C$_2$H$_5$)$_2$	682.80	87	0.62	−12.9
LVI	BocD-LPR-ANSNHC$_3$H$_7$	748.94	82	0.68	−35.5
LVII	D-LPR-ANSNHC$_3$H$_7$·2HCl	721.74	93	0.50	−50.1
LVIII	(N^a-Boc,N^w-Z)KR-ANSN-(CH$_3$)$_2$	768.93	87	0.59	−6.3
LIX	(N^w-Z)KR-ANSN(CH$_3$)$_2$·2HCl	741.73	81	0.49	+15.4
LX	KR-ANSN(CH$_3$)$_2$·3HBr	777.43	82	0.28	+9.6
LXI	BzlGR-ANSNH(i-C$_3$H$_7$)	694.80	85	0.61	−19.4
LXII	TosGPR-ANSNH(i-C$_4$H39)	742.86	75	0.61	−38.0

[a] In 1-butanol–acetic acid–water 4:1:2. [b] Solvent is DMSO.

fitting initial rates of substrate hydrolysis to the Michaelis–Menten equation.

Activation of Factor IX by Tissue Factor/Factor VIIa. The activation of factor IX was evaluated by adding zymogen factor IX to a mixture of tissue factor, factor VIIa, and phospholipid vesicles according to the general methods of Lawson and Mann (1991). Reactions were carried out in 20 mM Hepes, 0.15 M NaCl, 5 mM $CaCl_2$, pH 7.4 (HBS), at 37 °C. After relipidation of tissue factor into phospholipid vesicles (PCPS), factor VIIa was added to the reaction system and the TF/VIIa/PCPS complex was assembled. Reactions were started by the addition of factor IX to the experimental system. The final concentration of components in the reaction were the following: tissue factor, 10 nM; factor VIIa, 10 nM; PCPS, 200 μM; and factor IX, 1.5 μM. Factor IXaβ formation was evaluated using a discontinuous assay format by removing designated reaction time points (100 μL) from the ongoing activation reaction and rapidly diluting each time point into 1.1 mL of 200 μM substrate LVII which had been preequilibrated in HBS buffer with 5 mM $CaCl_2$ at 37 °C. The rate of factor IXaβ formation was reported by the change in fluorescence which corresponded to the hydrolysis of the provided substrate over a 1-min interval for each reaction time point. The initial rate of substrate hydrolysis for each time was then compared to an identical reaction sample which was quenched in an equal volume of 50 mM EDTA, 2% SDS (w/v), 0.01 M Tris-HCl, 10% glycerol, 2% 2-mercaptoethanol (v/v), and analyzed by SDS–PAGE (Laemmli, 1970). 10% polyacrylamide gels were stained with Coomassie Brilliant Blue and destained by diffusion. The physical conversion of factor IX to factor IXaβ was then evaluated by scanning densitometry using a Microscan 1000 scanning densitometer (TRI Inc.) according to the methods of Lawson and Mann (1991).

Activation of Protein C. The rate of activation of protein C by thrombin in TBS at 22 °C was measured in a continuous assay system. Fluorescent substrate LIII and protein C were incubated together in TBS, and the background rate of substrate hydrolysis was recorded. Thrombin (25 nM final) was added to the reaction, and the change in fluorescent intensity over time was recorded. Rates of substrate hydrolysis were determined from the slopes of tangents to the progress curve taken at 1-min time intervals. Thrombin hydrolysis of substrate LIII was determined independently. The resulting corrected rates of substrate hydrolysis were converted to concentrations of APC by reference to an APC standard curve. This reference standard curve was linear with respect to varying the APC concentration (0.5–10 nM) using a fixed concentration of substrate (10 μM). Secondary plots of APC concentration vs time for each initial protein C concentration were constructed, where the slopes of these plots represent the

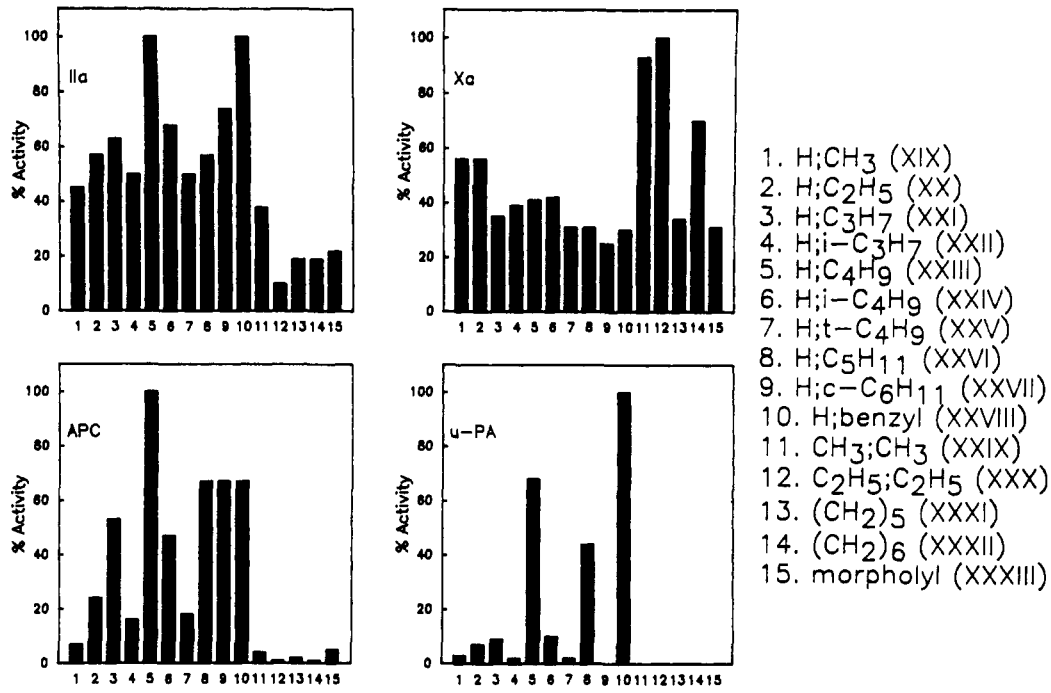

FIGURE 2: The relative activity of (N^{α}-Z)Arg-ANSNR$_1$R$_2$ with factor IIa, factor Xa, APC, and u-PA. The most reactive substrate for a particular enzyme was normalized to 100%. The activities of all other substrates were then calculated by dividing their initial rate of hydrolysis by the rate of hydrolysis of the most reactive substrate. In the case of monosubstituted cyclohexyl moieties and disubstituted analogues, the relative activity for u-PA was less than 1%.

initial rates of APC generation by IIa at each protein C concentration. Kinetic constants for protein C activation were determined using the nonlinear least-squares fitting program ENZFITTER as described above.

RESULTS

Physicochemical Characterization of the Synthesized ANSNs. Table I presents the structures and physicochemical constants of the fluorescent reporter groups used in this study and their relative fluorescent intensities. All of these compounds (IV–XVIII) and their precursors (I–III) are easily synthesized and purified to analytical grade by crystallization (compound VI is not crystalline). The compounds (IV–XVIII) have excitation maxima near 350 nm with emission maxima ranging from 465 to 476 nm. Fluorescent measurements show a 2.5-fold range (41–112) in the intensities of the fluorescent signals among the 15 synthesized compounds. Fluorogenic substrates (XIX–LXII; structure X-Arg-ANSNR$_1$R$_2$) show relative fluorescent intensities at 470 nm of less than 0.1% that of the respective free fluorophore. Detection of most of these fluorescent compounds at a concentration of 10^{-8} M can be easily achieved (>2× background) in the presence of 10^{-5} M fluorogenic substrate. Continuous excitation of any of these compounds at 352 nm for a period of 30 min resulted in no significant (<2%) deterioration of the fluorescence signal. Nonenzymatic hydrolysis rates in TBS at 4 °C were less than 0.2% in 30 days.

Physicochemical constants and the results of composition determinations for the blocked (N^{α}-carbobenzyloxy: XIX–XXXIII) and unblocked (XXXIV–LVIII) 6-(L-arginylamino)-1-naphthalenesulfonamide hydrobromides are reported in Tables II and III, respectively. Compounds reported in Table II were prepared from aminonaphthalenesulfonamides (IV–XVIII) and N^{α}-(carbobenzyloxy)-L-arginine hydrobromide with the synthesis carried out in pyridine. All of these compounds are crystalline and are of analytic grade.

Table IV presents the physicochemical characteristics of a set of 6-(peptidylamino)-1-naphthalenesulfonamides. Peptide substrates were all synthesized with relatively high yields (68–96%) using the general scheme outlined in Figure 1. N^{α}-Blocked peptides substrates (XLIX, LI, LIII, LV, LVI, LVIII, LXI, and LXII) have solubilities in aqueous buffer of at least 150 μM; peptide substrates unblocked at the N^{α} position (L, LII, LIV, LVII, LIX, and LX) have solubilities in the range of 1–3 mM.

Analysis of the N^{α}-Z-Blocked (Arginylamino)-naphthalenesulfonamides as Substrates for Various Enzymes. Table V reports hydrolysis data for eight enzymes for a series (XIX–XXXIII) of N^{α}-blocked (arginylamino)naphthalenesulfonamides each distinguished by substitutions on the fluorescent reporting group (R$_1$, R$_2$). The complementary series of unblocked compounds (XXXIV–XLVIII, see Table III) was also evaluated and in each case were hydrolyzed more slowly than the respective Z-blocked analogues. In general, the Z-blocked (arginylamino)naphthalenesulfonamides are relatively good substrates for Xa, IIa, and APC while being poorly hydrolyzed by Lys-plasmin and rt-PA. From Table V, it can be seen that three of the eight enzymes (IIa, APC, and u-PA) more rapidly hydrolyze the substrates in which the aminonaphthalenesulfonamide moiety is monosubstituted (R$_1$ = H). Figure 2 illustrates the relative activity of these substrates for IIa, Xa, APC, and u-PA as a function of increasing bulk of the alkyl side chains. These data demonstrate that, with monoalkylated detecting groups, rates of hydrolysis by IIa, APC, and u-PA increase with increasing length of linear alkyl chains, attaining a maximum rate with 4 methylenes (XXIII, R$_2$ = C$_4$H$_9$). Monoalkylated detecting groups with branched alkyl chains (XXI vs XXII; XXIII vs XXIV, XXV) show decreased rates of hydrolysis by IIa, APC, and u-PA. The activity of factor Xa toward these substrates, while comparable in magnitude to that of IIa and APC, appears generally less sensitive to structural variations in the detecting group.

Specific instances can be seen where substitutions result in significantly different hydrolysis rates both for a given enzyme and between enzymes. For example, IIa, Xa, and APC show

Table V: Initial Rate[a] of (N^{α}-Z)Arg-ANSNR$_1$R$_2$[b] Hydrolysis

			enzymes[c]							
	R_1	R_2	IIa	Xa	APC	Plm	t-PA	u-PA	VIIa	IXa
XIX	H	CH_3	44	67	14	0.5	0.7	2.5	SH	SH
XX	H	C_2H_5	56	67	49	SH	0.7	6.2	SH	SH
XXI	H	C_3H_7	62	42	111	0.5	SH	7.6	SH	SH
XXII	H	i-C_3H_7	49	46	33	0.6	SH	1.3	SH	SH
XXIII	H	C_4H_9	98	49	208	3.0	1.2	60	SH	SH
XXIV	H	i-C_4H_9	67	51	98	0.5	SH	8.3	SH	SH
XXV	H	t-C_4H_9	49	37	37	0.9	SH	1.3	SH	SH
XXVI	H	C_5H_{11}	56	37	140	3.2	0.7	39	SH	SH
XXVII	H	cyclo-C_6H_{11}	72	30	140	1.5	SH	0.5	SH	SH
XXVIII	H	benzyl	98	36	140	5.0	3.3	88	SH	SH
XXIX	CH_3	CH_3	37	111	8.3	1.5	SH	SH	SH	SH
XXX	C_2H_5	C_2H_5	10	119	1.5	0.6	SH	SH	SH	SH
XXXI		$(CH_2)_5$	19	41	4.6	1.4	SH	SH	SH	SH
XXXII		$(CH_2)_6$	19	83	2.0	1.1	SH	SH	SH	SH
XXXIII		morpholyl	22	37	9.7	0.7	SH	SH	SH	SH

[a] Rates given are in units of nM/(s nM enzyme) × 10^5. [b] Substrate concentration was 1 μM. [c] Concentration of enzyme was 100 nM. SH = slow hydrolysis (less than 0.5 × 10^{-5} nM/(s nM)).

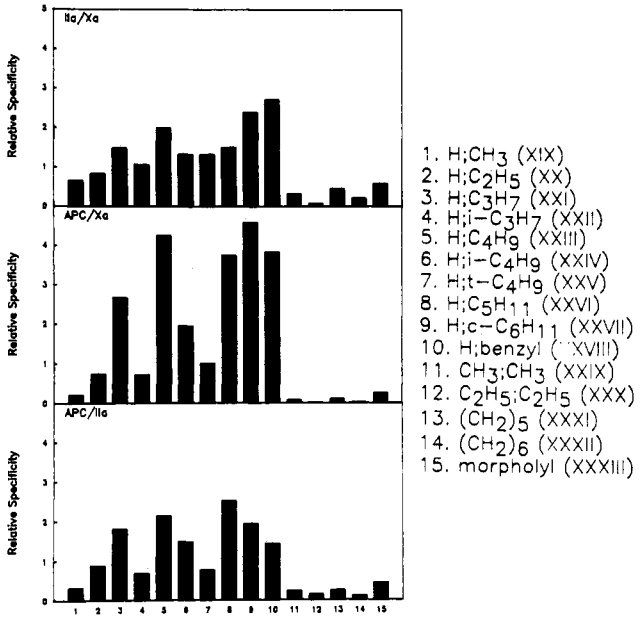

FIGURE 3: The relative specificity of (N^{A}-Z)Arg-ANSNR$_1$R$_2$ for factor IIa, factor Xa, and APC. The initial rate of hydrolysis for each substrate by a particular enzyme was divided by the initial rate of hydrolysis for the same substrate by the second enzyme.

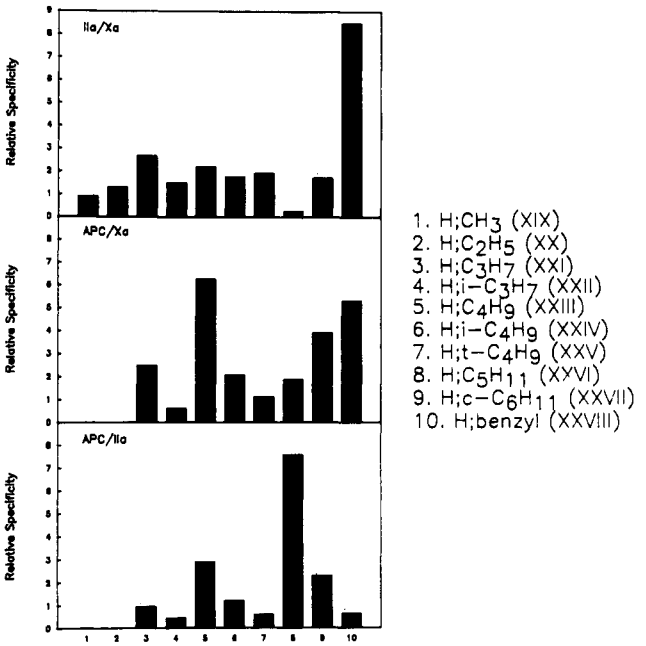

FIGURE 4: The relative specificity of (N^{α}-Z)Arg-ANSNR$_1$R$_2$ for factor IIa, factor Xa, and APC. Data are plotted as the k_{cat}/K_M of individual substrate for a particular enzyme divided by k_{cat}/K_M of the same substrate for a second enzyme. Data were not obtained for APC/Xa and APC/IIa when R_2 = CH_3 or C_2H_5 due to limited substrate hydrolysis such that full kinetic evaluation of substrate hydrolysis was not possible.

roughly equivalent rates of hydrolysis for compound XX (R^1 = H, R_2 = C_2H_5). When C_2H_5 is substituted at the R_1 and R_2 position (see compound XXX), the rate of hydrolysis by IIa decreases 6-fold, that of APC by about 33-fold, while the Xa-catalyzed hydrolysis rate increases 2-fold. K_M and k_{cat} values for the hydrolysis of a number of these compounds by IIa, Xa, and APC are presented in Table VI and in general confirm the patterns observed in Table V.

Figures 3 and 4 illustrate the relative specificity of various alkyl side chain modifications for pairs of enzymes (factor IIa vs factor Xa, APC vs factor Xa, and APC vs factor IIa). In general, these data are similar to the data presented in Figure 2 where substrate hydrolysis by the enzymes evaluated shows a distinct dependence on the structure of the substituents in the detecting group. These data demonstrate that the specificity of IIa/Xa is relatively insensitive to changes in alkyl side chain bulk. When the same series of ANSNs were evaluated for APC/Xa specificity, it was observed that the n-butyl side chain had the highest specificity for APC. When the selectivity of APC relative to IIa was evaluated, it was observed that the 5 carbon side chain group (C_5H_{11}) provided the most specificity for APC with respect to IIa.

Analysis of 6-(Peptidylamino)-1-naphthalenesulfonamides as Substrates for Various Enzymes. An evaluation of the suitability of the 6-(peptidylamino)-1-naphthalenesulfonamides (XLIX–LXII) as substrates for eight enzymes involved in blood coagulation and fibrinolysis is summarized in Table VII. This table demonstrates that the aminonaphthalenesulfonamides, when conjugated to a variety of peptide sequences, can function as sensitive detectors of enzymatic activity. Several of these substrates show promise for the measurement of either specific coagulation and fibrinolytic proteases or processes involving zymogen activation. For example, compound LV is hydrolyzed by factor VIIa (Lawson et al., 1992). Compound LV, LVI and LVII react with factor IXaβ, and compound LVI is hydrolyzed by plasmin 120 times faster than by urokinase.

A kinetic analysis of substrate hydrolysis by four of the enzymes (IIa, Xa, IXa, and APC) with eleven of these sub-

Table VI: Kinetic Constants[a] for the Hydrolysis of (N^{α}-Z)Arg-ANSNR$_1$R$_2$

	substrates			enzymes[b]		
	R_1	R_2		IIa	Xa	APC
XIX	H	CH_3	K_M	62.5	160	SH
			k_{cat}	0.04	0.11	
			k_{cat}/K_M	640	714	
XX	H	C_2H_5	K_M	171	121	SH
			k_{cat}	0.14	0.08	
			k_{cat}/K_M	820	636	
XXI	H	C_3H_7	K_M	22.2	125	320
			k_{cat}	0.04	0.07	0.47
			k_{cat}/K_M	1580	593	1470
XXII	H	i-C_3H_7	K_M	25	102	343
			k_{cat}	0.03	0.08	0.17
			k_{cat}/K_M	1180	800	510
XXIII	H	C_4H_9	K_M	32.4	139	171
			k_{cat}	0.04	0.08	0.62
			k_{cat}/K_M	1260	576	3600
XXIV	H	i-C_4H_9	K_M	35.3	86.5	960
			k_{cat}	0.05	0.07	1.6
			k_{cat}/K_M	1420	811	1670
XXV	H	t-C_4H_9	K_M	24	114	738
			k_{cat}	0.02	0.06	0.4
			k_{cat}/K_M	930	487	540
XXVI	H	C_5H_{11}	K_M	41.4	36.8	436
			k_{cat}	0.01	0.04	0.8
			k_{cat}/K_M	242	979	1830
XXVII	H	cyclo-C_6H_{11}	K_M	27.9	51.8	180
			k_{cat}	0.03	0.03	0.44
			k_{cat}/K_M	1090	633	2470
XXVIII	H	benzyl	K_M	41	213	218
			k_{cat}	0.07	0.04	0.23
			k_{cat}/K_M	1680	198	1050
XXIX	CH_3	CH_3	K_M	22.6	91.4	SH
			k_{cat}	0.01	0.09	
			k_{cat}/K_M	630	1020	
XXX	C_2H_5	C_2H_5	K_M	SH	200	SH
			k_{cat}		0.26	
			k_{cat}/K_M		1290	
XXXI		$(CH_2)_5$	K_M	SH	64.9	SH
			k_{cat}		0.06	
			k_{cat}/K_M		924	
XXXII		$(CH_2)_6$	K_M	SH	427	SH
			k_{cat}		0.13	
			k_{cat}/K_M		293	
XXXIII		morpholyl	K_M	SH	80	SH
			k_{cat}		0.05	
			k_{cat}/K_M		625	

[a] Units: K_M, μM; k_{cat}, s^{-1}; k_{cat}/K_M, M^{-1} s^{-1}. SH = slow substrate hydrolysis: no kinetic constants were calculated.

Table VII: Initial Rate[a] of Peptidyl-ANSNR$_1$R$_2$[b] Hydrolysis

		enzymes							
	substrates	IIa[d]	Plm[d]	VIIa[d]	IXa[e]	Xa[d]	APC[d]	u-PA[e]	t-PA[e]
XLIX	BocPFR-ANSNHC$_3$H$_7$	69	13	SH	SH	31	93	5.6	SH
L	PFR-ANSNHC$_3$H$_7$	56	21	SH	SH	222	1111	4.6	SH
LI	BocPPR-ANSNHC$_5$H$_{11}$	9259	3.5[e]	SH	SH	1.0[e]	111	43	0.4
LII	PPR-ANSNHC$_5$H$_{11}$	4630	9.3[e]	SH	SH	0.7[e]	1111	56	0.7
LIII	ZGGRR-ANSNH(cyclo-C$_6$H$_{11}$)	3.0	5.9	SH	SH	SH	463	SH	SH
LIV	GGRR-ANSNH(cyclo-C$_6$H$_{11}$)	3.0	11[e]	SH	SH	0.6[e]	560	1.2	SH
LV	MesD-LGR-ANSN(C$_2$H$_5$)$_2$	842	278	69	0.8	27778	56[e]	14	14
LVI	BocD-LPR-ANSNHC$_3$H$_7$	200000	3620	SH	3.5	646	3968	1614	1852
LVII	D-LPR-ANSNHC$_3$H$_7$	100000	815	SH	6.2	319	63291	688	712
LVIII	(N^{α}-Boc,N^{w}-Z)KR-ANSN(CH$_3$)$_2$	15	19[e]	SH	SH	1.2[e]	2.5[e]	SH	SH
LIX	(N^{w}-Z)KR-ANSN(CH$_3$)$_2$	11	19[e]	SH	SH	SH	5.1[e]	SH	SH
LX	KR-ANSN(CH$_3$)$_2$	SH	3.5[e]	SH	SH	SH	3.5[e]	SH	SH
LXI	BzIGR-ANSNH(i-C$_3$H$_7$)	694	14[e]	SH	SH	617	46	14	4.6
LXII	TosGPR-ANSNH(i-C$_4$H$_9$)	277778[c]	1111	SH	0.7	5556	13890	2800	14

[a] Data are normalized to nM/(s nM enzyme) × 10^5. [b] Substrate concentration was 1 μM. The remaining footnotes represent enzyme concentrations of 1 nM (*c*), 10 nM (*d*), and 100 nM (*e*). SH = slow hydrolysis (less than 0.4 × 10^{-5} nM/(s/nM).

strates is presented in Table VIII. In general, the ranges of observed K_M values (4–800 μM) and of k_{cat} values (0.0006/s to 50/s) are comparable to reported values for tripeptide substrates with different detecting groups (Lottenberg et al., 1981). In all cases but one (compound LXII with APC), the K_M values are below the solubility limits of the substrates, thus allowing at least 50% saturation of the target catalyst.

A comparison between the commercially available substrate chromozyme TH (TosGPR-pNA) and a peptidylamino-naphthalenesulfonamide with the same peptide sequence

Table VIII: Kinetic Constants[a] for Hydrolysis of Peptidyl-ANSNs

	substrates	kinetic constants	IIa	Xa	IXa	APC
XLIX	BocPFR-ANSNHC$_3$H$_7$	k_{cat}	0.04	0.06	SH	0.058
		K_M	44.4	230		37
		k_{cat}/K_M	900	260		1580
L	PFR-ANSNHC$_3$H$_7$	k_{cat}	0.36	1.33	SH	4.7
		K_M	600	667		240
		k_{cat}/K_M	600	2000		19600
LI	BocPPR-ANSNHC$_5$H$_{11}$	k_{cat}	1.39	0.00064	SH	0.16
		K_M	10.9	19		64
		k_{cat}/K_M	128000	34		2460
LII	PPR-ANSNHC$_5$H$_{11}$	k_{cat}	30.3	0.0023	SH	14.3
		K_M	667	27		640
		k_{cat}/K_M	45000	84		22300
LIII	ZGGRR-ANSNH(cyclo-C$_6$H$_{11}$)	k_{cat}	0.02	0.0052	SH	6.2
		K_M	12.5	29		320
		k_{cat}/K_M	1560	180		19300
LIV	GGRR-ANSNH(cyclo-C$_6$H$_{11}$)	k_{cat}	0.011	0.0091	SH	3.1
		K_M	30	56		267
		k_{cat}/K_M	350	160		11600
LV	MesD-LGR-ANSN(C$_2$H$_5$)$_2$	k_{cat}	0.63	36.4	0.033	0.055
		K_M	31.3	12.5	96	113
		k_{cat}/K_M	20000	291000	347	490
LVI	BocD-LPR-ANSNHC$_3$H$_7$	k_{cat}	29.4	3.8	0.03	4.7
		K_M	10.5	238.2	1.8	16.8
		k_{cat}/K_M	2.8×10^6	16000	16667	210000
LVII	D-LPR-ANSNHC$_3$H$_7$	k_{cat}	111.0	1.1	0.21	52.3
		K_M	3.8	40.3	3.3	44.9
		k_{cat}/K_M	28.9×10^6	27000	63115	1.16×10^6
LXI	BzIGR-ANSNH(i-C$_3$H$_7$)	k_{cat}	1.8	0.44	SH	0.055
		K_M	320	55.2		52
		k_{cat}/K_M	5600	7970		1070
LXII	TosGPR-ANSNH(i-C$_4$H$_9$)	k_{cat}	52.6	2.4	0.3	120
		K_M	11	35.3	123	800
		k_{cat}/K_M	4.8×10^6	68000	2400	150000

[a] Units: K_M, μM; k_{cat}, s^{-1}; k_{cat}/K_M, s^{-1} M^{-1}. SH = slow substrate hydrolysis; no kinetic constants were calculated.

Table IX: Comparison of the Fluorescent Detecting Groups

		maximum		assay condition[a]	
detecting groups	λ_{ex} (nm)	λ_{em} (nm)	F[b]	λ_{em} (nm)	F[b]
7-amino-4-methylcoumarin	380	440	5.5	460	3.8
2-naphthlamine	360	410	0.36	420	0.3
2-naphthol	320	360	0.34	420	0.16
6-amino-1-naphthalenecyclohexyl-sulfonamide[c]	352	470	1.0	470	1.0

[a] Reported emission wavelengths used for assays. [b] Relative fluorescence intensity in TBS, 25 °C. [c] Average detecting group for aminonaphthalenesulfonamides.

Table X: Comparison of Chromozyme TH (TosGPR-p-NA) with TosGPR-ANSNH(i-C$_4$H$_9$)

		enzyme	
substrate	kinetic constants	IIa	Xa
chromozyme TH	K_M (μM)	13.8	364
	k_{cat} (s^{-1})	14.1	244
	k_{cat}/K_M (M^{-1} s^{-1})	1.02×10^6	0.67×10^6
TosGPR-ANSNH(i-C$_4$H$_9$)			
	K_M (μM)	10.5	132
	k_{cat} (s^{-1})	45.6	11.2
	k_{cat}/K_M (M^{-1} s^{-1})	4.34×10^6	8.48×10^4

(LXII) is presented in Table X. Kinetic analysis of the hydrolysis of the two substrates by IIa yields similar K_M values with compound LXII showing a 4.3-fold greater catalytic efficiency. The catalytic efficiency of Xa hydrolysis of the tripeptide-*p*-nitroanilide, characterized by larger K_M and k_{cat} values than those of IIa, is similar to that of IIa. However, Xa hydrolysis of compound LXII is 50 times less efficient than that of IIa. Collectively these data provide evidence that the structure of the P′ detecting group contributes to the specificity of the enzyme substrate interaction.

Utility of Specific Peptide Substrates for Evaluating Zymogen Activation. As reported above, specific substrates were identified which exhibited reactivity with factors VIIa, IXaβ, and activated protein C. Specific examples of the utility of these substrates to investigate the activity or activation of these proteins are described below.

Factor VIIa. Substrate LV (MesD-LGR-ANSN(C$_2$H$_5$)$_2$) was observed to have significant reactivity with factor VIIa. To date, no fluorescent substrate has been identified which reacts with factor VIIa, and in general few synthetic substrates are hydrolyzed by factor VIIa (Zur & Nemerson, 1978; Kam et al., 1990; Pederson et al., 1990; Ruf et al., 1991) at rates which permit their practical application. Due to the fluorescent nature of the ANSN reporter group, the hydrolysis of substrate LV by factor VIIa is easily detected at factor VIIa concentrations below 10^{-9} M in the presence of 100 μM substrate, HBS buffer, and 5 mM $CaCl_2$. We have also observed that the enzymatic hydrolysis of substrate LV by factor VIIa is enhanced >100 times (k_{cat}/K_M) in the presence of saturating concentrations of tissue factor, allowing for the detection of factor VIIa activity in the presence of tissue factor at concentrations below 10^{-10} M. This substrate exhibited no reactivity with single-chain factor VII, supporting the conclusion that single-chain factor VII is a zymogen. A detailed analysis of the process of factor VIIa complex assembly with tissue factor and phospholipid has recently been reported (Lawson et al., 1992).[4]

Activation of Factor IX by Tissue Factor/Factor VIIa. Factor IXaβ has been difficult to evaluate in purified reaction

[4] A copy of this manuscript was enclosed for the reviewers' inspection.

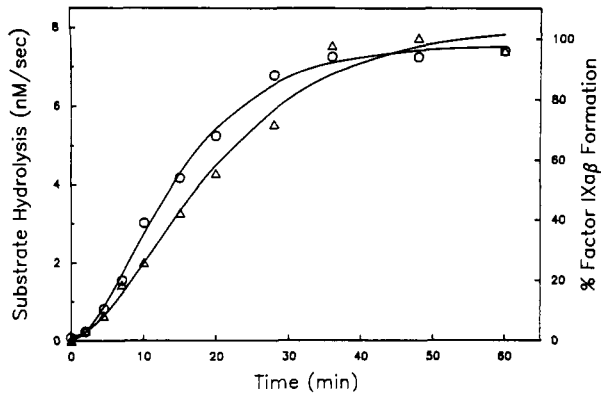

FIGURE 5: The activation of human factor IX by recombinant human factor VIIa/tissue factor. Data were obtained in a discontinuous assay format by removing reaction subsamples of factor IX activation at the following time points: 0, 2, 4, 5, 7, 10, 15, 20, 28, 36, 48, and 60 min after the addition of factor IX to the reaction system. Reaction aliquots were evaluated by rapidly diluting the subsample (100 μL) into 1.1 mL of buffer containing substrate LVII (D-LPR-ANSNHC$_3$H$_7$) (200 μM) and the rate of fluorescent substrate hydrolysis for each sample was determined (Δ). The concentrations of reagents used in this experiment were the following: factor IX, 1.5 μM; rVIIA, 10 nM; TF/PCPS, 10 nM/200 μM in HBS at 37 °C. An identical reaction subsample was removed from the experimental system and rapidly quenched in EDTA and prepared for SDS-PAGE. After electrophoresis, gels were stained with Coomassie Brilliant Blue and subjected to scanning densitometry. The percent of factor IXaβ formed was plotted as a function of time (○).

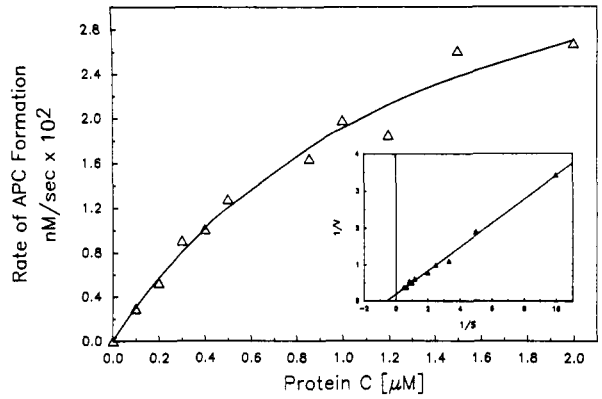

FIGURE 6: The kinetics of bovine protein C activation by factor IIa in the presence of substrate LIII (ZGGRR-ANSNH(cyclo-C$_6$H$_{11}$)). The concentration of reagents used in this experiment were the following: protein C, 0.1, 0.2, 0.3, 0.4, 0.5, 0.857, 1.0, 1.2, 1.5, 2.0 μM; factor IIa, 25 nM; substrate LIII, 10 μM.

systems due to its low amidolytic activity with short synthetic peptide substrates. Furthermore, the use of *p*-nitroanilides or amides of 7-amino-4-methylcoumarins in evaluating factor IXaβ activity has been limited due to very slow rates of substrate hydrolysis. The esterase activity of factor IXaβ is much higher, and the use of synthetic peptide esters (Byrne & Castellino, 1978; Byrne et al., 1980) and thioesters (McRae et al., 1981; Cho et al., 1984) has been reported. In the present study, four substrates were identified which exhibited significant reactivity with factor IXaβ (LV, LVI, LVII, and LXII). The kinetic constants of substrate hydrolysis of these four compounds are presented in Table VIII. The utility of substrate LVII in evaluating the activation of factor IX by the tissue factor/factor VIIa complex was investigated. Data presented in Figure 5 demonstrate the activation of factor IX by the tissue factor/factor VIIa enzymatic complex. This figure illustrates the increase in the rate of substrate hydrolysis as factor IX is converted to factor IXaβ during the activation process. Furthermore, these data demonstrate that the change in fluorescence observed during the reaction process correlates well with the physical conversion of factor IX to factor IXaβ as evaluated by SDS-PAGE. The sigmoidal shape of the fluorescent substrate hydrolysis curve is consistent with previous reports of factor IX activation by the tissue factor/factor VIIa complex, in which factor IX requires two proteolytic steps to be activated to the enzymatic product factor IXaβ (Bajaj et al., 1983; Lawson & Mann, 1991). Thus, the lag in initial fluorescent substrate hydrolysis occurs due to the first proteolytic step in the activation process, the conversion of factor IX to IXα, a nonenzymatic intermediate in the reaction process.

Activation of Protein C by Thrombin. Data presented in Table VIII demonstrate that substrate LIII exhibits a 12-fold advantage in catalytic efficiency for APC with respect to IIa. This advantage in catalytic efficiency for APC with respect to IIa was exploited to evaluate the activation of protein C by thrombin in a continuous assay. Figure 6 presents a kinetic analysis of the activation of protein C by thrombin using substrate LIII. The resulting kinetic constants for this process were calculated, yielding a K_M value of 1.4 μM, k_{cat} of 0.046 s^{-1}, and and overall catalytic efficiency of (k_{cat}/K_M) of 3.3 × 10^4 M^{-1} s^{-1}. These data were not corrected for the partitioning of thrombin between substrate LIII and protein C. This results in an underestimate of the kinetic efficiency of thrombin activation of protein C. However, in spite of this complexity, our data are in general agreement with a previous report (Amphlett et al., 1981) (K_M = 1.8 μM, k_{cat} = 0.009 s^{-1}) using a discontinuous system with benzoylarginine ethyl ester as the substrate. These data demonstrate that by identifying substrates with kinetic specificity (APC to IIa) the ANSN compounds can be used in a continuous assay format to evaluate various processes of zymogen activation.

Discussion

This report presents the synthesis of a new class of fluorescent detecting groups, the 6-amino-1-naphthalenesulfonamides (ANSN), for substrates of amidases. The general synthesis described allows for a wide range of chemical modifications of ANSN to be readily accomplished. Thus, the preparation of a series of structurally unique detecting groups with relatively constant fluorescent intensity is facilitated. These modifications of the detecting group can be used to enhance both the chemical (solubility and stability in aqueous buffer) and biological (reactivity with specific enzymes) properties of the synthesized substrates. The data presented illustrate that modifications of these detecting groups have significant influences upon the rate of substrate hydrolysis by various blood coagulation and fibrinolytic enzymes. From these data we show that both the P (peptidyl) and P′ (substrate leaving group) confer specificity to substrate interactions with this class of serine protease enzymes.

The fluorescent compounds described represent disubstituted bicyclic aromatic naphthalene rings maintaining a nucleophilic substituent (amino group) in the β-position of one aromatic ring and an electrophilic substituent (sulfonamide group) in the α-position of the other aromatic ring. The location of these substituents allows for a relatively high yield of fluorescence from the disubstituted naphthalenes.[5] The presence of a sulfonyl moiety in these detecting groups permits a large range of chemical modifications. Thus, any compound possessing primary or secondary amino groups, including amino acids or their derivatives, can be used to modify the detecting group.

[5] S. Butenas, unpublished observation, 1991.

Various modifications can be made which are able to compensate for the high hydrophobicity of the aromatic rings, thereby increasing the solubility of the detecting groups in water, and potentially increasing the overall solubility of the substrate.

When the ANSN detecting groups are compared with the more commonly used fluoresent detecting group 7-amino-4-methylcoumarin (Table IX), both detecting groups have a high yield of fluorescence. However, 7-amino-4-methylcoumarin has limited possibilities for modification due to the absence of a functional group(s) for this purpose. Thus, it is very difficult to modify this compound in order to optimize the enzyme substrate interaction or to modulate the solubility of the overall substrate.

The modifiability of the ANSN compounds has allowed us to make systematic changes in the alkyl side chain of the substrate leaving group. These data (Table V) demonstrate that three of these enzymes (IIa, APC, and u-PA) more rapidly hydrolyze substrates with monosubstituted sulfonamide moieties in the detecting group (R_1 = H). Furthermore, these data demonstrate a dependence between the bulk of the linear alkyl chain at the R_2 position and the rate of substrate hydrolysis observed. Generally, an increase in the rate of substrate hydrolysis is observed with increasing length of the alkyl side chain, attaining a maximum with the *n*-butyl homologue (XXIII, $R_2 = C_4H_9$). Further increases in alkyl chain length results in decreased rates of substrate hydrolysis. These data suggest that the structure of the P′ group has a significant influence upon substrate–enzyme interaction. Likely explanations for this include both steric and electrostatic interactions of the substrate as it sits in the enzyme active site pocket.

When Z-blocked arginyl-ANSNs with branched monoalkyl side chains in the detecting groups were evaluated, it was observed that the substrates with branched side chains were hydrolyzed more slowly by the enzymes studied in this report (XXI vs XXII; XXIII vs XXIV, XXV). It was also observed that as the alkyl side chain branching increased the rate of substrate hydrolysis decreased further (XXIII–XXIV–XXV). However, the dependence of the activity of IIa, APC, and u-PA on the structure of substituents in the detecting group is different for each enzyme. For factor IIa, the difference between the maximum and the minimum rate of hydrolysis in this group of substrates (XIX–XXVI) is 2.2-fold (XXIII vs XIX). For APC it is 15-fold (XXIII vs XIX), and for u-PA it is 45-fold (XXIII vs XXII or XXV).

It is interesting to compare these data to the reactivity of the same compounds with factor Xa (Figure 2). Factor Xa hydrolyzes substrates with short alkyl chains (XIX, XX) faster than those with longer alkyl side chains. However, there is little difference in the rate of hydrolysis among homologues with linear and branched alkyl side chains. These data would suggest that the S′ region of the active site pocket of factor Xa is less discriminating with respect to subtle changes in the bulk of short chain substitutions of the ANSN leaving group. When the disubstituted compounds (XXIX, XXX) were evaluated, it was observed that these substrates were more rapidly hydrolyzed by factor Xa than their monosubstituted analogues (XIX, XX).

When substrates possessing monosubstituted sulfonamide moieties with cyclic structures (XXVII, XXVIII) were evaluated, these compounds exhibited significant reactivity for IIa, Xa, APC, and u-PA. These data suggest that both steric and electronic characteristics of the cyclic rings contribute to the reactivity of the substrate for the S′ region of the active site pocket. These compounds were hydrolyzed at almost the same rate (except the cyclohexyl analogue by u-PA) as the compound with the *n*-butyl substitution (XXIII) which was in general the optimal linear alkyl side chain. Possible explanations for the reactivity of the aromatic substituent include the relatively small size of the planar aromatic ring, its ability to take sterically favorable positions by rotation around the aliphatic bond, and/or specific electronic characteristics of the ring optimizing the enzyme substrate interaction. The relatively large cyclohexyl ring in the detecting group (XXVII) is hydrolyzed in the same range as the aromatic analogue (XXVIII) by factor IIa, Xa, and APC. However u-PA, t-PA, and Lys-plasmin exhibit a substantial decrease in substrate hydrolysis when presented with substrates with the larger ring size at the P′ position. These data suggest that u-PA, t-PA, and Lys-plasmin have limitations to the size of ring groups which can be substituted on the ANSN moiety and still allow for efficient enzymatic hydrolysis.

Collectively, our data illustrate that, for the 8 enzymes evaluated above, alterations in the P′ site of the substrate have significant influence upon the specificity of the enzyme–substrate interactions. Thus, one of the utilities of ANSN is that it allows for modifications in the substrate leaving group. Such modifications can provide structural information regarding the active site pocket of various enzymes by changes in both the bulk and electrostatic properties of the detecting group. The utility of modifying substrate leaving groups to add both sensitivity and specificity for a particular enzyme is an area of ongoing investigation in our laboratory.

When the 6-(peptidylamino)-1-naphthalenesulfonamide substrates were screened for reactivity with various serine protease enzymes (Table VII), it was observed that many of these substrates were rapidly hydrolyzed by thrombin, factor Xa, Lys-plasmin, and APC. These data would suggest that the active site pocket of these enzymes can accept a fairly high degree of modification in the P_2 and P_3 position and still allow for significant substrate hydrolysis.

Table X presents a specific case in which a modification in the substrate detecting group increases the specificity of the enzyme substrate interaction. This table compares the kinetic constants of thrombin and factor Xa substrate hydrolysis for two identical tripeptide substrates (TosGPR-p-NA and TosGPR-ANSNH(i-C_4H_9). These data demonstrate that a particular modification in the ANSN detecting group increases the kinetic specificity (k_{cat}/K_M) more than 30 times (IIa/Xa) compared to that of the analogous p-NA compound. Thus, highly specific and sensitive substrates for various proteases may be developed by optimizing the appropriate P (peptidyl) sequences for maximal reactivity with a particular enzyme and by modifying the ANSN structure to optimize the reactivity of the P′ substrate leaving group as it interacts with the enzyme active site pocket.

Lastly, we have been able to exploit both the sensitivity and specificity of the peptidyl ANSN compounds to identify specific cases of reactive substrates for factor VIIa, IXaβ, and APC. To date, few substrates have been identified which exhibit significant reactivity for factor VIIa (Zur & Nemerson, 1978; Kam et al., 1990; Pederson et al., 1990; Ruf et al., 1991). We have exploited the sensitivity and reactivity of substrate LV (MesD-LGR-ANSN(C_2H_5)$_2$) with factor VIIa to evaluate changes in the enzymatic activity of factor VIIa as a function of complex assembly with tissue factor (Lawson et al., 1992).

Assays for factor IXaβ have been accomplished using ester or thioester substrates (McRae et al., 1981; Cho et al., 1984). N^{α}-Benzoyl-L-arginine ethyl ester has also been used as a substrate for IXaβ (Byrne et al., 1980); however this compound

is a poor substrate (K_M = 27 mM) and has limited utility in a multienzyme system due to its broad specificity. McRae et al. (1981) reported the activity of IXaβ toward several thioester substrates but also reported that the utility of these compounds was limited due to the inhibition of factor IXaβ by free thiols in the reaction system. We have identified four substrates which reacted with factor IXaβ (LV, LVI, LVII, and LXII). Of these substrates LVII appeared to have the most useful properties for evaluating factor IX activation by the tissue factor/factor VIIa complex. These properties of substrate LVII included a high degree of solubility in aqueous buffer and a low degree of reactivity with factor VIIa. These data (Figure 5) demonstrate that substrate LVII is a useful tool to analyze the activation process of factor IX by the tissue factor/factor VIIa complex.

The study of the process of protein C activation by thrombin in a continuous assay system has been difficult due to the lack of selectivity in the available synthetic substrates for APC with respect to thrombin. Discontinuous assay systems which rely upon the introduction of thrombin inhibitors at timed intervals have been reported (Ohno et al., 1981; Haley et al., 1989). Substrate LIII has been used to monitor the activation of protein C, by thrombin, in a continuous assay format. The resulting kinetic constants (K_M = 1.4 μM, k_{cat} = 0.046 s^{-1}) are in reasonable agreement with a previous report (Amphlett et al., 1981) (K_M = 1.8 μM, k_{cat} = 0.009 s^{-1}) using a discontinuous system with benzoylarginine ethyl ester as the substrate. These data suggest that the presence of the peptidyl-ANSN in the reaction mixture had little effect on the kinetics of protein C activation by thrombin under the assay conditions described above. However, because substrate LIII is hydrolyzed by thrombin it is not the ideal reporter group for continuous assays of protein C by thrombin.

The structure activity analysis presented provides a potential approach to the synthesis of a more specific substrate. For example, the monosubstituted pentyl-ANSN achieves the greatest advantage in catalytic efficiency for APC over IIa. We feel that these data provide insight into structural alterations which can be made on both the peptidyl (P) and detecting group (P′) side of the substrate to further optimize the specificity of the substrate for use in a continuous assay system with a mixture of proteases.

ACKNOWLEDGMENTS

We are grateful to co-workers of Dr. Saulius Butenas of the Institute of Biochemistry, Vilnius, Lithuania for participation in the construction of peptides used for substrate synthesis. We are grateful to Dr. Ulla Hedner of Novo Nordisk Pharmaceuticals for providing recombinant human factor VIIa. We are grateful to Dr. Shu-Len Liu of Baxter Healthcare Corp. for providing recombinant human tissue factor. We are grateful to Dr. Steve Olsen for providing purified factor XIa, which was used to activate factor IX to IXa. We thank Natalie Ribarik for excellent technical assistance in the preparation of various proteins used in this study.

REFERENCES

Amphlett, G. W., Kisiel, W., & Castellino, F. J. (1981) *Biochemistry 20*, 2156–2161.

Anderson, G. W., Zimmerman, J. E., & Callahan, F. U. (1964) *J. Am. Chem. Soc. 86*, 1838–1842.

Bajaj, S. P., Rapaport, S. I., & Brown, S. F. (1981) *J. Biol. Chem. 256*, 253–259.

Barlow, G. H., Summaria, L., & Robbins, K. C. (1984) *Biochemistry 23*, 2384–2387.

Bell, P. H., Dziobkowski, C. T., & Englert, M. E. (1974) *Anal. Biochem. 61*, 200–208.

Byrne, R., & Castellino, F. J. (1978) *Arch. Biochem. Biophys. 190*, 687–692.

Byrne, R., Link, R. P., & Castellino, F. J. (1980) *J. Biol. Chem. 255*, 5336–5341.

Cho, K., Tanaka, T., Cook, R. R., Kisiel, W., Fujikawa, K., Kurachi, K., & Powers, J. C. (1984) *Biochemistry 23*, 644–650.

Claeys, H., Molla, A., & Verstraete, M. (1973) *Thromb. Res. 3*, 515–523.

Esmon, C. T., Stenflo, J., Suttie, J. W., & Jackson, C. M. (1976) *J. Biol. Chem. 251*, 3052–3057.

Fujikawa, K., & Davie, E. W. (1976) *Methods Enzymol. 45*, 89–95.

Haley, P. E., Doyle, M. F., & Mann, K. G. (1989) *J. Biol. Chem. 264*, 16303–16309.

Higgins, D. L., & Mann, K. G. (1983) *J. Biol. Chem. 258*, 6503–6508.

Kam, C., Vlasuk, G. P., Smith, D. E., Arcuri, K. E., & Powers, J. C. (1990) *Thromb. Haemostasis 64*, 133–137.

Kisiel, W., & Davie, E. W. (1981) *Methods Enzymol. 80*, 320–332.

Kisiel, W., Hermodson, M. A., & Davie, E. W. (1976) *Biochemistry 15*, 4901–4906.

Kisiel, W., Canfield, W. M., Ericsson, L. H., & Davie, E. W. (1977) *Biochemistry 16*, 5824–5831.

Klein, J. D., & Walker, F. J. (1986) *Biochemistry 25*, 4175–4179.

Krishnaswamy, S., Church, W. R., Nesheim, M. E., & Mann, K. G. (1987) *J. Biol. Chem. 262*, 3291–3399.

Laemmli, U. K. (1970) *Nature 227*, 680–685.

Lawson, J. H., & Mann, K. G. (1991) *J. Biol. Chem. 266*, 11317–11327.

Lawson, J. H., Butenas, S., & Mann, K. G. (1992) *J. Biol. Chem. 267*, 4834–4843.

Lindquist, P. A., Fujikawa, K., & Davie, E. W. (1978) *J. Biol. Chem. 253*, 1902–1909.

Lottenberg, R., Christensen, U., Jackson, C. M., & Coleman, P. L. (1981) *Methods Enzymol. 80*, 341–361.

Lundblad, R. L., Kingdon, H. S., & Mann, K. G. (1976) *Methods Enzymol. 45*, 156–176.

Mann, K. G., Elion, J., Butkowski, R. J., Downing, M., & Nesheim, M. E. (1981) *Methods Enzymol. 80*, 286–302.

McRae, B. J., Kurachi, K., Heimark, R. L., Fujikawa, K., Davie, E. W., & Powers, J. C. (1981) *Biochemistry 20*, 7196–7206.

Morita, T., Kato, H., Iwanaga, S., Takada, K., Kimura, T., & Sakakibara, S. (1977) *J. Biochem. 82*, 1495–1498.

Nieuwenhuizen, W., Wijngaards, G., & Groeneveld, E. (1977) *Anal. Biochem. 83*, 143–148.

Ohno, Y., Kato, H., Morita, T., Iwanaga, S., Takada, K., Sakakibara, S., & Stenflo, J. (1981) *J. Biochem. 90*, 1387–1395.

Pedersen, A. H., Lund-Hansen, T., Bisgaard-Frantzen, H., Olsen, F., & Petersen, L. C. (1989) *Biochemistry 28*, 9331–9336.

Pedersen, A. H., Nordfang, O., Norris, F., Wiberg, F. C., Christensen, P. M., Moeller, K. B., Meidahl-Pedersen, J., Bech, T. C., Norris, K., Hedner, U., & Kisiel, W. (1990) *J. Biol. Chem. 265*, 16786–16793.

Rijken, D. C., & Collen, D. (1981) *J. Biol. Chem. 256*, 7035–7041.

Ruf, W., Rehemtulla, A., & Edgington, T. S. (1991) J. Biol. Chem. 266, 2158–2166.
Schechter, I., & Berger, A. (1967) Biochem. Biophys. Res. Commun. 27, 157.
White, W. F., & Barlow, G. H. (1970) Methods Enzymol. 19, 665–672.
Zur, M., & Nemerson, Y. (1978) J. Biol. Chem. 253, 2203–2209.

Conformational Properties of the G·G Mismatch in d(CGCGAATTGGCG)$_2$ Determined by NMR†

Katherine L. B. Borden,‡ Terence C. Jenkins,§ Jane V. Skelly,§ Tom Brown,∥ and Andrew N. Lane*,‡

Laboratory for Molecular Structure, National Institute for Medical Research, The Ridgeway, Mill Hill, London NW7 1AA, U.K., Cancer Research Campaign Biomolecular Structure Unit, Institute of Cancer Research, Sutton, Surrey SM2 5NG, U.K., and Department of Chemistry, University of Edinburgh, Edinburgh EH9 3JJ, U.K.

Received October 28, 1991; Revised Manuscript Received March 18, 1992

ABSTRACT: The conformational properties of the DNA duplex d(CGCGAATTGGCG)$_2$, which contains two noncomplementary G·G base pairs, have been examined in aqueous solution by ^{1}H and ^{31}P NMR as a function of temperature. The G·G mismatch is highly destabilizing, with a T_m value 35 K below that observed for the native *Eco*RI dodecamer. The dodecamer appears symmetric in the NMR spectra and exists largely as an average B-type DNA conformation. However, the ^{1}H and ^{31}P NMR spectra give evidence of considerable conformational heterogeneity at the mismatched nucleotides and their nearest neighbors, which increases with increasing temperature. There is no evidence for a significant population of the syn purine conformation. The imino protons of the mispaired bases G4 and G9 are degenerate, resonate at high field, and exchange readily with solvent. These results indicate that the mispaired bases are only weakly hydrogen-bonded and are only partially stacked into the helix. On raising the temperature, the duplex shows increasing exchange between two or more conformations originating from the mismatch sites. However, these additional conformations maintain their Watson–Crick hydrogen bonding. The increase in chemical exchange is consistent with a quasimelting process for which the G·G sites provide local nuclei. Extensive modeling studies by dynamic annealing have confirmed that the G(anti)·G(anti) conformation is favored and that the mispairs are poorly stacked within the helix. The results explain both the poor thermal stability and low hypochromicity of this duplex.

The limited fidelity of DNA polymerase is responsible for the relatively frequent [frequency of occurrence is $\sim 10^{-4}$; see review by Loeb and Kunkel (1982)] formation of noncomplementary base pairs during DNA synthesis. Such mismatches provide intermediates in the mutagenic pathway. To maintain the integrity of the genetic information mistakes that occur during replication must be repaired with high efficiency. The overall fidelity of replication is $\sim 10^{-10}$ errors per nucleotide (Fowler et al., 1974). Of the possible base mispairings, purine·purine and purine·pyrimidine pairs occur more frequently than pyrimidine·pyrimidine pairs (Topal & Fresco, 1976; Fersht & Knill-Jones, 1981). If uncorrected, purine·purine mismatches lead to transversions in the daughter strands, e.g., A·T → A·A$_{syn}$ → T·A; G·C → G·G$_{syn}$ → C·G (Topal & Fresco, 1976). Cellular repair mechanisms require effective recognition of the mismatch sites prior to base correction. Three major factors affect the detection of a mismatch base pair: (i) the structure of the mispairing, (ii) the nature of the adjacent base sequences, and (iii) the conformation of the DNA in the vicinity of the lesion. The relative repair efficiencies for base-pair mismatches are in the order A·C, G·G, G·T > A·A > A·G, C·C, C·T, T·T (Kramer et al., 1984). Further, the A·G repair efficiency is very sensitive to the base composition of the surrounding sequence, in particular the A·T versus G·C content, which is mirrored by the sensitivity of the mismatch conformation to the flanking sequences (Kramer et al., 1984; Dohet et al., 1985). There are also differences in repair efficiency within the purine·purine class, with G·G > A·A > A·G. Although the chemical structures of these mismatches are different, the ability of the cellular repair enzymes to detect these errors may also depend on the different conformations available to the DNA, for example, the possibility of hydrogen-bonding patterns in A·G pairings that are not available in G·G mismatches.

In the class of purine·purine mismatches, A·G mispairs have been studied extensively by both NMR and X-ray crystallography (Gao & Patel, 1988; Brown et al., 1990; Webster et al., 1990; Carbonnaux et al., 1991; Lane et al., 1991b), and NMR studies have also been reported for A·A (Arnold et al., 1987), AP·A (Fazakerley et al., 1986), and A·I mismatches (Uesugi et al., 1987). However, only comparatively little is known about the G·G mispairing. ^{31}P NMR studies (Roongta et al., 1990) and preliminary ^{1}H NMR experiments (Piotto & Gorenstein, 1991) have recently been reported for a G·G-mismatched dodecamer duplex. Topal and Fresco (1976) suggested that the G·G mismatch would pair using one base in the keto form and syn and the other in the enol form and anti. However, Cognet et al. (1991) have presented evidence

† This work was supported by the Cancer Research Campaign, the Medical Research Council, and the Science and Engineering Research Council of the U.K.
‡ National Institute for Medical Research.
§ Institute of Cancer Research.
∥ University of Edinburgh.

0006-2960/92/0431-5411$03.00/0